AJNR

MR of the submandibular gland: normal and pathologic states.

T Kaneda, M Minami, K Ozawa, Y Akimoto, T Kawana, H Okada, H Yamamoto, H Suzuki and Y Sasaki

AJNR Am J Neuroradiol 1996, 17 (8) 1575-1581
http://www.ajnr.org/content/17/8/1575

MR of the Submandibular Gland: Normal and Pathologic States

Takashi Kaneda, Manabu Minami, Kaoru Ozawa, Yoshiaki Akimoto, Tomonori Kawana, Hiroyuki Okada, Hirotsugu Yamamoto, Hiromi Suzuki, and Yasuhito Sasaki

PURPOSE: To evaluate the MR appearance of normal and pathologic states of the submandibular gland. **METHODS:** MR images of 22 healthy subjects and 21 patients with histopathologically confirmed disorders of the submandibular gland (five pleomorphic adenomas, two hemangiomas, two malignant lymphomas, one adenoid cystic carcinoma, one squamous cell carcinoma, and 10 cases of sialadenitis) were reviewed. **RESULTS:** All normal submandibular glands showed higher signal intensity than surrounding muscle but lower intensity than fat on T1-weighted and T2-weighted images. Postcontrast images showed moderate enhancement of the gland. All the tumors had lower signal intensity than the normal submandibular gland on T1-weighted images and had intermediate to high (n = 8) or high (n = 3) signal intensity relative to the normal submandibular gland on T2-weighted images. Six of seven benign tumors were well defined, and three of four malignant tumors were poorly defined. In all cases of sialadenitis, the submandibular gland showed diffusely different signal intensities from the normal gland on both T1-weighted and T2-weighted images. Eight cases of chronic sialadenitis showed lower T2-weighted signal intensities than the normal gland, and this can be explained histopathologically by marked fibrosis and cellular infiltration. **CONCLUSIONS:** MR imaging can show the presence, extent, margins, and signal intensity changes of pathologic conditions of the submandibular gland.

Index terms: Salivary glands, magnetic resonance; Salivary glands, neoplasms

AJNR Am J Neuroradiol 17:1575–1581, September 1996

The submandibular gland is the second largest salivary gland, about half the size of the parotid gland (1). Eighty percent of all salivary gland tumors arise in the parotid gland, 10% in the submandibular gland, and the remaining 10% in the minor salivary gland and sublingual gland (2). The proportion of malignant tumors differs among the various salivary glands. In the parotid gland, about 20% of all tumors are malignant, whereas in the submandibular gland, 45% are malignant (2). Moreover, the submandibular gland is susceptible to stone formation, inflammation, and sialectasia because the direction of salivary flow is against gravity. Therefore, the differential diagnosis among benign and malignant neoplasms and inflammation is important for patients with problems in the submandibular gland.

Magnetic resonance (MR) imaging can delineate various kinds of soft tissues clearly with high contrast resolution. Recently, MR imaging has been used in the diagnosis of many pathologic conditions of the parotid gland (3–7). The purpose of this study was to evaluate MR findings depicting normal and pathologic states of the submandibular gland and to correlate the MR findings with histopathologic observations.

Materials and Methods

We reviewed the MR images of the submandibular gland obtained in 12 women and 10 men (mean age, 42 years; range, 22 to 54 years) who were examined by precontrast and postcontrast MR imaging for various problems of the face and neck not related to the submandibular gland or to the floor of the mouth. These problems included odontogenic cysts in the maxilla (11 patients), maxillary sinusitis (five patients), and postoperative max-

Received June 6, 1995; accepted after revision February 22, 1996.

From the Departments of Radiology (T.Kan., K.O., H.S.), Oral Surgery (Y.A.,T.Kaw.), and Pathology (H.O., H.Y.), Nihon University School of Dentistry at Matsudo, Chiba, and the Department of Radiology, University of Tokyo Hospital, Tokyo (M.M.,Y.S.), Japan

Address reprint requests to Takashi Kaneda, DDS, PhD, Department of Radiology, Nihon University School of Dentistry at Matsudo, 2–870–1, Sakaecho-Nishi, Matsudo, Chiba 271, Japan.

AJNR 17:1575–1581, Sep 1996 0195-6108/96/1708–1575

illary cysts (six patients). The submandibular gland in these patients was considered to be representative of that in healthy subjects from the viewpoint of clinical signs and symptoms and radiologic findings. The signal intensities of the gland were compared with those of fat and muscle on T1-weighted images and with those of cerebrospinal fluid and muscle on T2-weighted images.

Separately, 34 patients with suspected submandibular gland lesions have been studied prospectively with MR imaging since March 1992. Their clinical symptoms included swelling (n = 12), pain (n = 12), and painless palpable masses (n = 10) in the submandibular region. Among them, 21 patients whose diagnoses were confirmed pathologically by specialists in oral pathology were chosen for this study. This group comprised 14 women and seven men (mean age, 51 years; range, 18 to 83 years). Fourteen of them had surgery or open biopsy, and seven had fine-needle aspiration biopsy after MR examinations. The pathologic specimens were classified according to guidelines established by the World Health Organization (8).

MR examinations were performed on a 0.2-T permanent magnet system with a head coil. Axial T1-weighted images were obtained using the spin-echo technique. The scanning parameters were as follows: 363/20/2 (repetition time/echo time/excitations), 256 × 256 matrix, 300 × 300-mm field of view, 7-mm section thickness, and 8.4-mm section interval. Axial T2-weighted images were also acquired using the spin-echo technique at 3000/120, with other parameters identical to those for T1-weighted images. In addition, coronal or sagittal T1-weighted images were obtained with the same pulse sequence as that used for axial T1-weighted images. In 10 of 21 cases, enhanced studies were performed with the same sequence as the precontrast T1-weighted images after intravenous injection of 10 mL (5 mmol) of gadopentetate dimeglumine.

MR signal intensity and its heterogeneity of the normal submandibular gland were evaluated by two radiologists on T1-weighted, T2-weighted, and postcontrast T1-weighted images. MR images of the pathologic lesions in the submandibular gland were evaluated by two radiologists in terms of presence, margination, heterogeneity of internal structures, T1-weighted and T2-weighted signal intensities, and contrast enhancement of the lesions before histopathologic examinations. The signal intensities of the lesions seen on T1-weighted and T2-weighted images were compared with those of normal submandibular gland tissue and other standards used in the healthy subjects. For this purpose, a five-point grading system was applied: on T1-weighted images, grade 1 represented almost the same signal intensity as muscle; grade 2, higher signal intensity than muscle and lower signal intensity than normal submandibular gland; grade 3, the lesion was isointense with the gland; grade 4, higher signal intensity than the normal submandibular gland and lower signal intensity than fat; and grade 5, almost the same signal intensity as fat. On T2-weighted images, grade 1 represented almost the same signal intensity as muscle; grade 2, higher signal intensity than muscle and lower signal intensity than normal submandibular gland; grade 3, the lesion was isointense with the gland; grade 4, the lesion and fat were isointense; and grade 5, almost the same signal intensity as cerebrospinal fluid.

Results

The normal submandibular gland (n = 44) appeared homogeneous (24/44) or heterogeneous (20/44) in signal intensity on both T1- and T2-weighted images. On both T1- and T2-weighted images, the signal intensity of the gland was higher than that of surrounding mus-

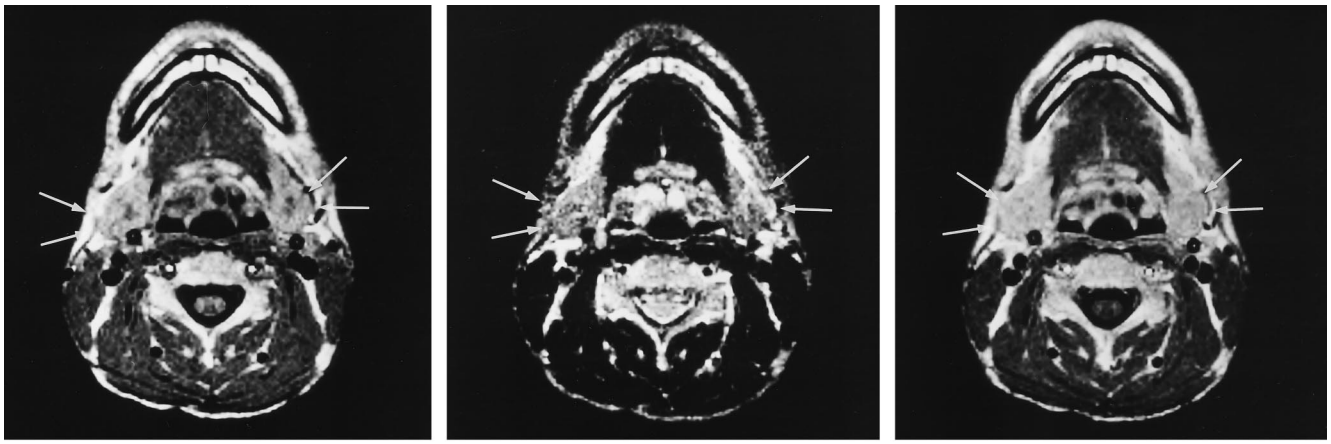

Fig 1. Normal submandibular gland in a 34-year-old man. The normal submandibular gland is higher in intensity than that of surrounding muscle but slightly lower than that of fat tissue (*arrows*) on both T1-weighted (*A*) and T2-weighted (*B*) MR images. The gland shows moderate enhancement (*arrows*) after contrast administration (*C*).

Histopathologic and MR imaging data of submandibular gland lesions in 21 cases

Patient	Age, y/Sex	Diagnosis	Margins	Heterogeneity	Signal Intensity Grade on T1-Weighted Images	Signal Intensity Grade on T2-Weighted Images	Degree of Contrast Enhancement
1	50/F	Pleomorphic adenoma	Well defined	Heterogeneous	1	4 to 5	+
2	43/F	Pleomorphic adenoma	Well defined	Heterogeneous	1	4 to 5	. . .
3	67/F	Pleomorphic adenoma	Well defined	Heterogeneous	1	4 to 5	+
4	48/M	Pleomorphic adenoma	Well defined	Heterogeneous	1	4 to 5	+
5	52/M	Pleomorphic adenoma	Well defined	Homogeneous	1	5	. . .
6	66/M	Hemangioma	Well defined	Heterogeneous	1	4 to 5	+ +
7	79/F	Hemangioma	Poorly defined	Heterogeneous	1	5	. . .
8	59/M	Malignant lymphoma	Poorly defined	Heterogeneous	2	4 to 5	±
9	33/F	Malignant lymphoma	Well defined	Heterogeneous	2	4 to 5	±
10	83/M	Adenoid cystic carcinoma	Poorly defined	Heterogeneous	1 to 2	3 to 4	. . .
11	67/F	Squamous cell carcinoma	Poorly defined	Heterogeneous	1 to 2	3 to 4	+
12	45/F	Acute sialadenitis	Well defined	Heterogeneous	1	4 to 5	. . .
13	51/F	Acute sialadenitis	Poorly defined	Heterogeneous	1	4 to 5	. . .
14	40/F	Chronic sialadenitis	Well defined	Heterogeneous	2	2 to 3	±
15	18/M	Chronic sialadenitis	Poorly defined	Heterogeneous	2	2 to 3	±
16	59/F	Chronic sialadenitis	Well defined	Homogeneous	2	2	. . .
17	53/F	Chronic sialadenitis	Well defined	Heterogeneous	2	2	. . .
18	28/M	Chronic sialadenitis	Well defined	Heterogeneous	1	2	. . .
19	42/F	Chronic sialadenitis	Well defined	Heterogeneous	1	2	. . .
20	50/F	Chronic sialadenitis	Well defined	Heterogeneous	2	2 to 3	. . .
21	43/F	Chronic sialadenitis	Well defined	Heterogeneous	1	2 to 3	. . .

Note.—+ + indicates strong; +, moderate; and ±, poor.

cle but lower than that of fat tissue. After administration of contrast material, the normal submandibular gland showed moderate homogeneous enhancement in all cases (Fig 1).

The pathologic diagnoses and MR imaging findings are summarized in the Table. Seven lesions were histopathologically diagnosed as benign tumors, four as malignant tumors, two as acute sialadenitis, and eight as chronic sialadenitis. All 11 tumors could be easily detected as focal abnormalities with sparing of some portions of normal parenchyma on MR images. They appeared as low signal intensity masses on T1-weighted images and intermediate to high (n = 8) or high (n = 3) signal intensity masses on T2-weighted images. Six of seven benign tumors were well defined. All pleomorphic adenomas appeared as well-defined masses, and three of them showed marginal lobulations (Fig 2). One of two hemangiomas and three of four malignant tumors had poorly defined margins. The MR findings on marginations were in close agreement with the histopathologic findings in all tumors. Heterogeneous internal architecture was found in six of seven benign tumors and in all malignant tumors, so heterogeneity of signal intensity was not useful for differentiating between benign and malignant tumors. In two cases, malignant lymphoma invaded the submandibular gland and was associated with lymphadenopathy surrounding the gland (Fig 3). Adenoid cystic carcinoma (Fig 4) and squamous cell carcinoma were not associated with lymphadenopathy in the current study.

In sialadenitis, the normal signal intensity of the submandibular gland was diffusely replaced on both T1- and T2-weighted images. All cases of acute sialadenitis had higher signal intensity than normal on T2-weighted images (Fig 5), whereas seven of eight cases of chronic sialadenitis had lower signal intensity than normal on T2-weighted images. Histopathologically, chronic sialoadenitis showed marked fibrosis and cellular infiltration (Fig 6).

Discussion

It is essential that the differential diagnosis establish whether a lesion is located within or outside the submandibular gland, because about half of all intraglandular tumors are malignant. Extraglandular lesions are mostly lymph node abnormalities and include metastasis and lymphoma as well as benign enlargement (2, 9). It is also critical for proper treat-

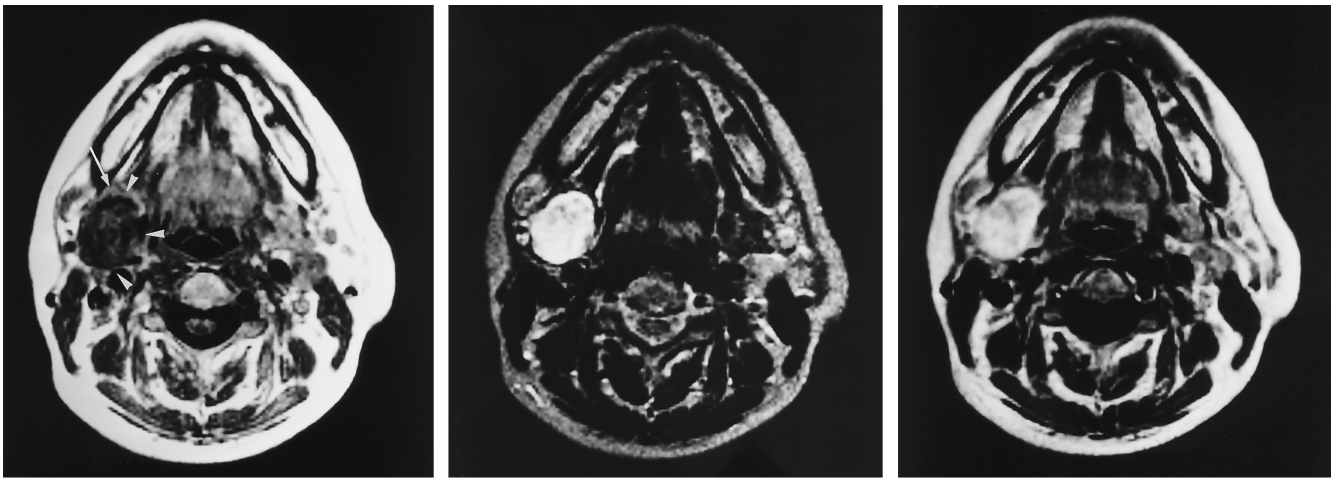

A B C

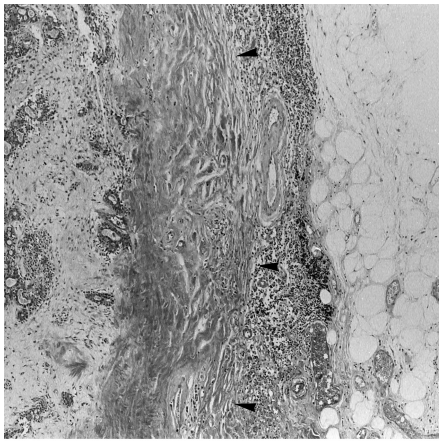

D

Fig 2. Pleomorphic adenoma in a 50-year-old woman.

A, Axial T1-weighted MR image shows a well-defined focal mass of heterogeneously low signal intensity, lower than normal submandibular gland, in the right submandibular gland (*arrowheads*). The residual glandular tissue is displaced medially (*arrow*).

B, On the T2-weighted image, the lesion appears well defined with heterogeneously high signal intensity. The lesion is isointense with fat.

C, On the postcontrast T1-weighted image, there is moderate enhancement in the lesion.

D, Pleomorphic adenoma was proved histopathologically, and photomicrograph shows it surrounded by a thin layer of fibrous connective tissue (*arrowheads*) (hematoxylin-eosin, original magnification ×10).

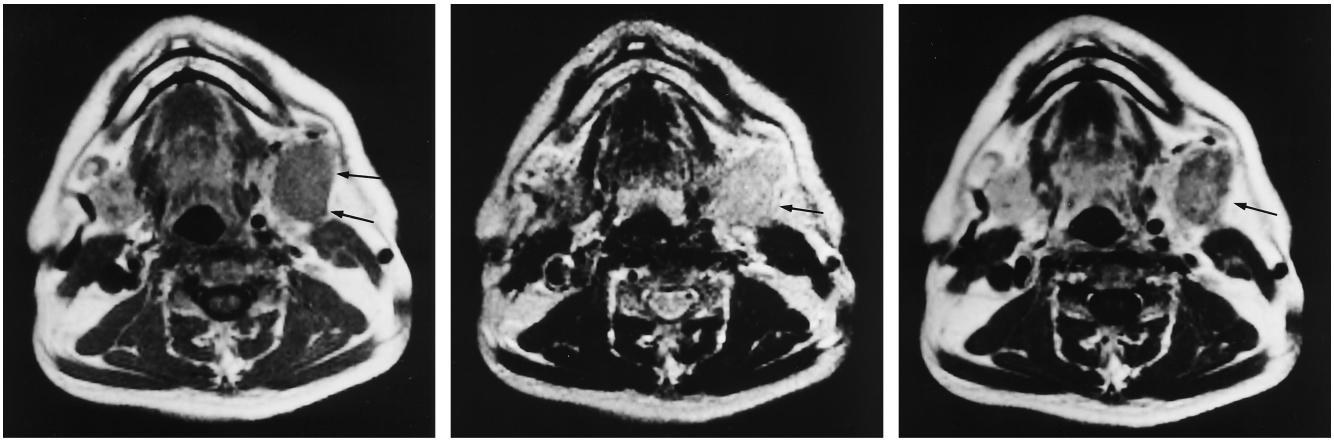

A B C

Fig 3. Malignant lymphoma in a 59-year-old man.

A, Axial T1-weighted MR image shows a poorly defined mass of low signal intensity in the left submandibular gland (*arrows*). Note small amount of normal gland medial to lesion.

B, On the T2-weighted image, the lesion is revealed as a heterogeneous mass of intermediate to high signal intensity (*arrow*).

C, Postcontrast T1-weighted image shows poor enhancement of the lesion (*arrow*) compared with normal portion of gland medially.

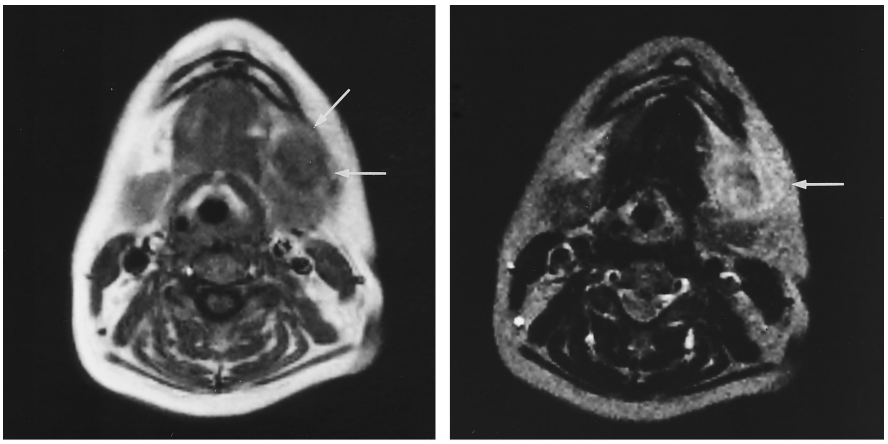

A B

Fig 4. Adenoid cystic carcinoma in an 83-year-old man.

A, Axial T1-weighted MR image shows a poorly defined mass (*arrows*) of low signal intensity in the left submandibular gland.

B, On the T2-weighted image, the lesion is revealed as a heterogeneous mass of intermediate to high signal intensity (*arrow*).

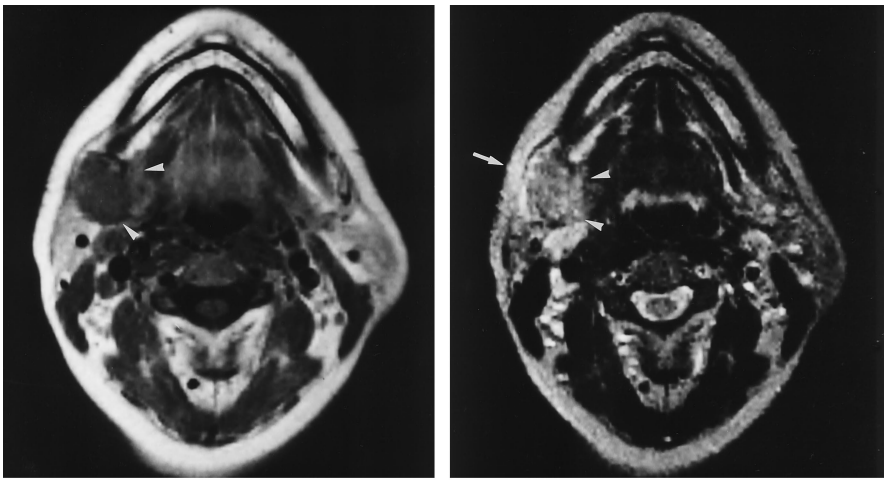

A B

Fig 5. Acute sialadenitis in a 45-year-old woman.

A, Axial T1-weighted MR image shows lower signal intensity entirely in the right (as compared with the left) submandibular gland (*arrowheads*).

B, On the T2-weighted image, the lesion appears intermediate to high in intensity (*arrowheads*). The periglandular tissue shows high signal intensity (*arrow*).

ment to define the lesion's extent in the submandibular region (9).

Sialography, which is the best method for visualizing the salivary ductal system, is an invasive examination (1). Computed tomography (CT) shows the submandibular gland as a structure of similar density to muscle (at 35 to 60 Hounsfield units), so evaluation of extension of disease around the gland is sometimes difficult (10). Yasumoto et al (11) reported that 27 of 35 submandibular gland tumors could not be seen clearly on precontrast CT scans. Sialographic CT can demonstrate the major ductal anatomy and intraglandular lesions as a defect, but is still invasive (12).

Concerning the frequency of malignant tumors in the submandibular gland, Spiro et al (13) reported that 96 (44%) of 217 tumors in their study were benign and 121 (56%) were malignant. The most frequently occurring benign lesions in that study were mixed tumors (43%). Eneroth et al (14) reported that among 157 submandibular gland tumors, 95 (61%) were benign and 62 (39%) were malignant. The three most common malignant tumors in both studies were adenoid cystic carcinoma (19% and 40%, respectively), mixed tumors (11% and 24%), and mucoepidermoid carcinomas (10% and 11%). In the current study, although the series of malignant tumors was slightly unusual and the total number was limited, all the neoplastic lesions had focal abnormalities of different signal intensity from that of the normal submandibular gland on T1-weighted or T2-weighted images, making the tumor extension in the gland distinct. However, MR imaging could not differentiate between benign and malignant tumors, and was not useful in histopathologic diagnosis. Seifert et al (2) reported that histopathologic criteria for malignant tu-

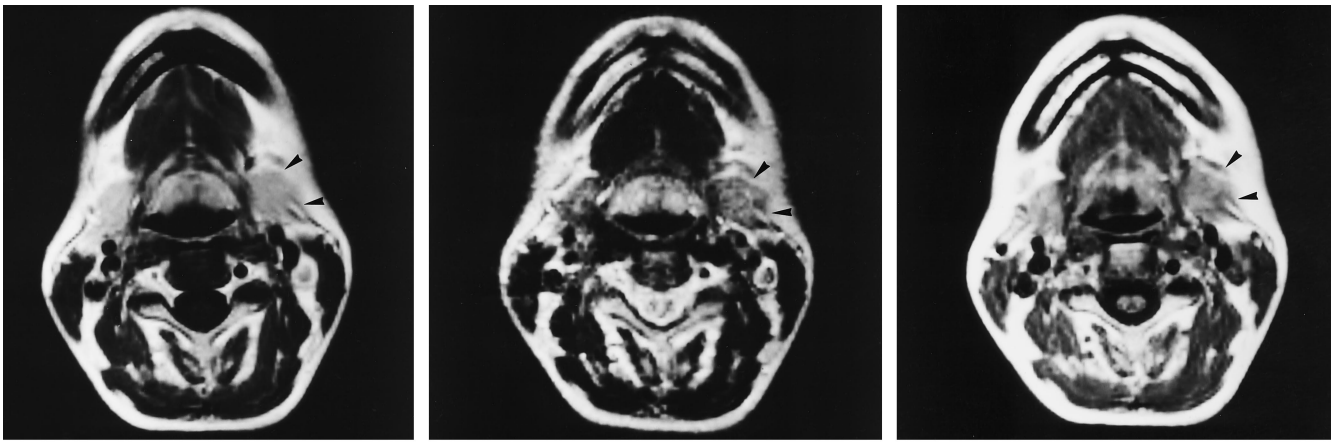

A B C

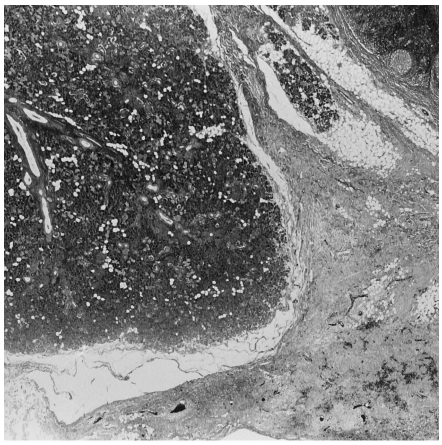

D

Fig 6. Chronic sialadenitis in an 18-year-old man.

The left submandibular gland shows lower signal intensity (*arrowheads*) on axial T1-weighted (*A*) and T2-weighted (*B*) images.

C, On postcontrast T1-weighted image, there was poor enhancement in the left submandibular gland (*arrowheads*).

D, Histopathologically, the lesion showed marked fibrosis and cellular infiltration (hematoxylin-eosin, original magnification ×10).

mors of the salivary gland include the presence of infiltration, vascular invasion, perineural spread, and metastasis. Mandelblatt et al (15) reported that the most reliable MR feature of malignant parotid gland tumors is poorly defined margins. In keeping with this observation, we found poorly defined tumor margins in nine of 11 cases of malignant tumor. Vogl et al (16) reported that postcontrast MR imaging was helpful in delineating tumorous lesions and in differentiating between benign and malignant lesions. However, another study found that even enhanced MR imaging could not differentiate malignant from benign lesions (17). In the current study, tumor enhancement was useful in delineating tumor extension, but clear differentiation between benign and malignant lesions was not possible, even on postcontrast images. Further research on this point will be necessary.

Clinically, painful enlargement of the submandibular gland may be produced by two different circumstances: inflammation or infection of the gland caused by ductal occlusion and infection not preceded by ductal obstruction (18). Isacsson et al (19) found that salivary calculi caused inflammation in the submandibular gland in 83% of patients who had pain in the region, and radiography was 92% accurate in the diagnosis of salivary calculi. In the present study, all patients with sialoadenitis had diffusely abnormal signal intensity in the submandibular gland, which was different from focal abnormalities of neoplasms. However, MR imaging is less sensitive than radiography and CT in detecting calcifications like sialolithiasis. In addition, chronic sialadenitis without sialolithiasis is often difficult to differentiate from such neoplasms as high-grade malignant tumors in clinical situations (20). At MR imaging, high-grade malignant tumors in the parotid gland are reported to show low T2-weighted signal intensity as well as poorly defined margins, making their appearance similar to chronic sialoadenitis if they replace the gland diffusely.

In conclusion, MR imaging was able to show an abnormality of the submandibular gland with different intensity from that of normal gland. Although the signal intensity itself is nonspecific, MR images showed the margins of the lesions, which correlated well with pathologic findings.

References

1. Som PM, Bergeron RT. *Head and Neck Imaging*. 2nd ed. St Louis, Mo: Mosby-Year Book; 1991:284–286
2. Seifert G, Miehlke A, Haubrich J, Chilla R. Diseases of the Salivary Glands: Pathology-Diagnosis-Treatment-Facial Nerve Surgery. Stuttgart, Germany: Thieme Verlag; 1986:5–6, 110–12, 171–291
3. Schaefer SD, Maravilla KR, Burns DK, Close LG, Merkel MA, Suss RA. Evaluation of NMR versus CT for parotid masses: a preliminary report. *Laryngoscope* 1985;95:45–950
4. Teresi LM, Lufkin RB, Wortham DG, Abemayor E, Hanafee WN. Parotid masses: MR imaging. *Radiology* 1987;163:405–409
5. Casselman JW, Mancuso AA. Major salivary gland masses: comparison of MR imaging and CT. *Radiology* 1987;165:183–189
6. Minami M, Tanioka H, Oyama K, et al. Warthin tumor of the parotid gland: MR-pathologic correlation. *AJNR Am J Neuroradiol* 1993;14:209–214
7. Joe VQ, Westesson PL. Tumors of the parotid gland: MR imaging characteristics of various histologic types. *AJR Am J Roentgenol* 1994;63:433–438
8. Seifert G. *Histological Typing of Salivary Gland Tumours*. 2nd ed. Berlin, Germany: Springer-Verlag; 1991:8–38
9. Batsakis JG. *Tumors of the Head and Neck: Clinical and Pathological Considerations*. 2nd ed. Baltimore, Md: Williams & Wilkins; 1979:1–75
10. Bryan RN, Miller RH, Ferreyro RI, Sessions RB. Computed tomography of the major salivary glands. *AJR Am J Roentgenol* 1982; 139:547–554
11. Yasumoto M, Shibuya H, Susuki S, et al. Computed tomography and ultrasonography in submandibular tumours. *Clin Radiol* 1992;46:114–120
12. Stone DN, Mancuso AA, Rice D, Hanafee WN. Parotid CT sialography. *Radiology* 1981;108:393–397
13. Spiro RH, Hajdu SI, Strong EW. Tumors of the submaxillary gland. *Am J Surg* 1976;132:463–468
14. Eneroth CM, Hjertman L, Moberger G. Malignant tumors of the submandibular gland. *Acta Otolaryngol* 1967;64:514–536
15. Mandelblatt SM, Braun IF, Davis PC, Fry SM, Jacobs LH, Hoffman JC Jr. Parotid masses: MR imaging. *Radiology* 1987;163:411–414
16. Vogl TJ, Dresel SH, Spath M, et al. Parotid gland: plain and gadolinium-enhanced MR imaging. *Radiology* 1990;177: 667–674
17. Chaudhuri R, Gleeson MJ, Graves PE, Bingham JB. MR evaluation of the parotid gland using STIR and gadolinium-enhanced imaging. *Eur Radiol* 1992;2:357–364
18. Wood NK, Goaz PW. *Differential Diagnosis of Oral Lesions*. 3rd ed. St Louis, Mo: Mosby; 1985:632–653
19. Isacsson G, Isberg A, Haverling M, Lundquist PG. Salivary calculi and chronic sialoadenitis of the submandibular gland: a radiographic and histologic study. *Oral Surg* 1984;58:622–627
20. Som PM, Biller HF. High-grade malignancies of the parotid gland: identification with MR imaging. *Radiology* 1989;173:823–826